

RESEARCH

Open Access



Chromosome-level genome provides insights into environmental adaptability and innate immunity in the common dolphin (*delphinus delphis*)

Kui Ding^{1,2}, Qinzeng Xu^{1,2}, Liyuan Zhao³, Yixuan Li^{1,2}, Zhong Li^{1,2}, Wenge Shi^{1,2}, Qianhui Zeng³, Xianyan Wang^{3*} and Xuelei Zhang^{1,2,4*}

Abstract

The common dolphin (*Delphinus delphis*) is widely distributed worldwide and well adapted to various habitats. Animal genomes store clues about their pasts, and can reveal the genes underlying their evolutionary success. Here, we report the first high-quality chromosome-level genome of *D. delphis*. The assembled genome size was 2.56 Gb with a contig N50 of 63.85 Mb. Phylogenetically, *D. delphis* was close to *Tursiops truncatus* and *T. aduncus*. The genome of *D. delphis* exhibited 428 expanded and 1,885 contracted gene families, and 120 genes were identified as positively selected. The expansion of the HSP70 gene family suggested that *D. delphis* has a powerful system for buffering stress, which might be associated with its broad adaptability, longevity, and detoxification capacity. The expanded IFN- α and IFN- ω gene families, as well as the positively selected genes encoding tripartite motif-containing protein 25, peptidyl-prolyl cis-trans isomerase NIMA-interacting 1, and p38 MAP kinase, were all involved in pathways for antiviral, anti-inflammatory, and antineoplastic mechanisms. The genome data also revealed dramatic fluctuations in the effective population size during the Pleistocene. Overall, the high-quality genome assembly and annotation represent significant molecular resources for ecological and evolutionary studies of *Delphinus* and help support their sustainable treatment and conservation.

Keywords *Delphinus delphis*, Genome sequencing, Chromosome assembly, Comparative genomics, Demographic history

*Correspondence:

Xianyan Wang
wangxianyan@tio.org.cn
Xuelei Zhang
zhangxl@fio.org.cn

¹Key Laboratory of Marine Eco-Environmental Science and Technology, First Institute of Oceanography, Ministry of Natural Resources, Qingdao, China

²Laboratory for Marine Ecology and Environmental Science, Qingdao Marine Science and Technology Center, Qingdao, China

³Key Laboratory of Marine Ecological Conservation and Restoration, Third Institute of Oceanography, Ministry of Natural Resources, Xiamen, China

⁴National Engineering Laboratory for Integrated Aero-Space-Ground-Ocean Big Data Application Technology, Xi'an, China



© The Author(s) 2024. **Open Access** This article is licensed under a Creative Commons Attribution 4.0 International License, which permits use, sharing, adaptation, distribution and reproduction in any medium or format, as long as you give appropriate credit to the original author(s) and the source, provide a link to the Creative Commons licence, and indicate if changes were made. The images or other third party material in this article are included in the article's Creative Commons licence, unless indicated otherwise in a credit line to the material. If material is not included in the article's Creative Commons licence and your intended use is not permitted by statutory regulation or exceeds the permitted use, you will need to obtain permission directly from the copyright holder. To view a copy of this licence, visit <http://creativecommons.org/licenses/by/4.0/>. The Creative Commons Public Domain Dedication waiver (<http://creativecommons.org/publicdomain/zero/1.0/>) applies to the data made available in this article, unless otherwise stated in a credit line to the data.

Introduction

The common dolphin (*Delphinus delphis*), recognized as one of the most widely distributed small cetaceans, inhabits seas ranging from temperate to tropical regions globally [1, 2]. Characterized by pelagic habitats [3, 4], these dolphins exhibit remarkable diving abilities, reaching depths up to 200 m [4], and demonstrate exceptional mobility, capable of covering over 500 km within days [5–7]. Notably, their strong adaptability is reflected in their diverse diet and resilience to environmental changes, as evidenced by recent studies on genotype-environment associations [8–10]. Despite their position at the top of the marine food chain, which subjects them to biomagnification of pollutants, common dolphins show no significant effects from contaminant accumulation [11–13]. Common dolphins, characterized as K-strategists—species that allocate substantial resources towards nurturing a smaller number of offspring over extended lifespans—are believed to have a lifespan ranging from 25 to 30 years [6, 14]. Research utilizing logistic regression methods has determined the onset of sexual maturity and initial reproductive age to be approximately 8.24 and 9.23 years, respectively [15]. Moreover, the duration of their reproductive phase is estimated to span 10 to 20 years [11, 16, 17]. Their resilience, coupled with their K-strategist reproductive strategy, underscores the need for further research into their immune system and environmental adaptability.

The innate immune system, often heralded as the first barrier against pathogenic invasion, relies on a swift, non-specific mechanism encompassing cytokine interactions, pattern recognition receptors, the complement system, and a variety of immune cells tasked with pathogen identification and elimination [18, 19]. Despite considerable research efforts into the immunology of marine mammals over the past decades, our understanding of cetacean immune systems remains notably fragmented [20]. The lymphoid organs in cetaceans, subject to the impacts of infectious agents and inflammatory diseases, have seen epidemics and isolated instances of distemper-like illnesses across species, including common dolphins [20, 21]. The advent of comprehensive genome analysis has shed light on the significance of certain genes and pathways within cetacean immune responses, enriching our grasp of their immune defenses [22]. While instances of primary hematopoietic neoplasms and lymphoproliferative diseases are relatively rare in cetaceans [23], sporadic reports of malignant lymphoma have emerged in a limited number of dolphin species [24, 25]. In beluga whales, an uptick in neoplastic diseases linked to exposure to persistent organic pollutants hints at potentially compromised antitumoral immune responses or carcinogenic effects stemming from environmental contaminants [26, 27]. Nevertheless, it's important to highlight

that instances of neoplastic disease have yet to be identified in common dolphins.

Reference genomes serve as pivotal tools for delving into the evolutionary relationships, historical demographics, and the evolutionary journey of genes and traits within the animal kingdom [28]. Within the marine ecosystem, cetaceans hold a distinctive role, underscored by the assembly and publication of multiple reference genomes in recent years (e.g., *Delphinapterus leucas*, *Orcinus orca*, *T. truncatus*, *Physeter macrocephalus*, etc.), which have significantly advanced our grasp of their evolutionary narratives [29, 30]. These initiatives have paved the way for comparative genomic and evolutionary studies, broadening our comprehension of these exceptional marine inhabitants. Despite these advancements, there remains a gap in the availability of high-quality, chromosome-level genomes for several marine mammal species, essential for nuanced analyses of ecology and biological evolution [31–33].

This study presents the assembly and annotation of a high-quality, chromosome-level genome for the common dolphin (*D. delphis*), achieved through the synergistic application of Illumina sequencing, PacBio-circular consensus sequencing (CCS), and Hi-C technology. Our comparative genomic analyses offer new insights into the phylogenetic positioning, demographic history, and genetic traits pivotal for adaptation to marine environments and innate immunity. The unveiling of this well-annotated, high-caliber genome assembly not only propels forward comparative genomic research but also lays a solid foundation for biodiversity cataloging and supports informed conservation and management strategies for cetaceans.

Materials and methods

Sample collection and DNA and RNA extraction

On January 7, 2019, a male common dolphin (*D. delphis*, specimen ID Code Ddel79) was found stranded along the coast of Lianjiang, Fujian Province, China. This specimen, displaying a fresh odor, intact appearance with some superficial skin abrasions, and clear eyes, was determined to be less than 24 h post-mortem (classified as Code 2) [34]. It was promptly frozen for preservation and identified as a short-beaked common dolphin based on its physical characteristics [35] and mitochondrial DNA markers (*cox1* and *cytb*). We harvested fresh samples from the muscle, skin, heart, adipose tissue, liver, and brain. The muscle tissue was immediately flash-frozen in liquid nitrogen and stored at -80°C for DNA extraction. The other tissues were submerged in RNA preservation solution (Absin Bioscience Inc.) to maintain RNA integrity. The genomic DNA was extracted using the standard phenol-chloroform method and assessed for quality and integrity through 1% agarose gel electrophoresis, Qubit

4 (Invitrogen, USA), and Agilent qPCR (Mx3005P, USA). Only DNA samples that met high-quality standards were selected for library preparation. Total RNA was extracted from the remaining tissues using the RNeasy Mini Kit (Qiagen, Germany), in accordance with the manufacturer's instructions. The quality and integrity of the RNA were evaluated using Agilent qPCR. RNA samples with an RNA Integrity Number (RIN) of at least 5.3 and a total amount of at least 0.4 µg were selected for further transcription and library sequencing.

Library construction and sequencing

Short-insert paired-end (PE) (350 bp) DNA Illumina library was constructed according to manufacturer's instructions (Illumina, San Diego, California, US). Sequencing runs for the PE library were performed on the Illumina Novaseq 6000 platform. PacBio-CCS sequencing libraries were prepared using the SMRTbell Template Prep Kit 1.0-SPv3 according to standard protocols. The Hi-C library, targeting *D. delphis* muscle tissues, was constructed in alignment with the methodology outlined by Belton et al. (2012) [36], facilitating the achievement of a chromosome-level genome assembly. Furthermore, RNA sequencing was carried out on samples from five primary tissues of *D. delphis* to enhance the genome annotation process.

Genome assembly

The genome size, heterozygosity, and repeat rate of *D. delphis* were estimated using a K-mer approach ($k=17$) [37] based on the Jellyfish method [38]. To refine our estimates, we subsequently applied GenomeScope2 [39] for a more precise analysis. For assembly, we utilized long-read data with Hifiasm (v0.8-dirty-r280) [40] under default settings to generate contig sequences (*_p_ctg.fa). These sequences were further processed with Purge Haplotigs (v1.1.0) [41] to reduce heterozygosity by identifying and removing haplotigs based on low-coverage areas in the genome bam file derived from second-generation sequencing data, yielding optimized contig sequences.

To obtain valid Hi-C data, we aligned the contig sequences of the *D. delphis* genome using bowtie2 v2.4.2 [42] and hicup v0.8.1 [43]. Specifically, we selected reads near the enzyme digestion sites to facilitate the assembly process. Subsequently, the contig sequences were clustered, ordered, and oriented with ALLHiC v0.9.8 [40, 44], based on their Hi-C interaction data. Utilizing methodologies delineated in Howe et al., 2021 [45], and employing the Rapid Curation pipeline from the Sanger Institute (<https://gitlab.com/wtsi-grit/rapid-curation>), in conjunction with the published common dolphin whole-genome reference sequence from NCBI (GCF_949987515.1), the complete X chromosome and a partial Y chromosome of *D. delphis* were successfully assembled. Finally,

we manually adjusted the orientation and order of each chromosome using Juicebox to produce a chromosomal-level genome assembly.

To assess the completeness and accuracy of the genome assembly, 248 conserved genes from 6 eukaryotic model organisms were selected and subjected to the Core Eukaryotic Genes Mapping Approach (CEGMA v2.5) [46] analysis and the Benchmarking Universal Single-Copy Orthologs (BUSCO v4.1.2) [47] analysis. We then aligned the assembled genome against high-fidelity (HiFi) reads using Minimap2 [48] to determine the gene collapse rate and identify the extent of base collapse. Coverage depth was calculated using SAMtools v0.1.19 [49], and areas of significantly reduced coverage were pinpointed through a custom Python script. Furthermore, the assembly's Quality Value (QV) was quantified with Merqury [50], providing an additional measure of assembly integrity.

Genome annotation

To annotate the repetitive sequences in the *D. delphis* genome, we employed a dual strategy that combines both homology alignment and *de novo* prediction techniques. Tandem repeat elements were pinpointed using Tandem Repeats Finder v4.09 [51], which relies on ab initio prediction for identification. For homology-based alignments, we annotated transposable elements (TEs) using RepeatMasker version 4.0.7, alongside its internal tool RepeatProteinMask [52], by aligning sequences against the RepBase library v14.06 [53]. In parallel, for *de novo* prediction of repeats, tools such as LTR_Finder [54], RepeatModeler version 1.0.10 [55], and RepeatScout v1.0.5 (<http://www.repeatmasker.org/>) were utilized to construct a comprehensive *de novo* repeat library. This library was then applied to identify DNA-level repetitive sequences within the *D. delphis* genome, ensuring a thorough and accurate annotation of its repetitive elements.

For predicting protein-coding genes, a comprehensive automated gene prediction pipeline was implemented, utilizing multiple algorithms including Augustus v3.2.3 [56], Geneid v1.4 [46], Genescan v1.0 [57], GlimmerHMM v3.04 [58], and SNAP v2013-11-29 (<http://korflab.ucdavis.edu/software.html>). The sequences of homologous proteins were downloaded from the NCBI database and DNA Zoo (Table S1). These protein sequences were then aligned to the genome using tblastN v2.2.26 [59] with $E\text{-value} \leq 1e-5$. Subsequently, the matching proteins were aligned to their corresponding genomic sequences, with GeneWise v2.4.1 [60] facilitating the precise spliced alignments necessary for predicting gene structures within each protein-coding region. Additionally, RNA-seq reads were meticulously aligned to the assembled genome using Hisat v2.0.4 [61] to pinpoint exon regions and splice junctions. The outcomes of these

alignments served as crucial input for Cufflinks v2.2.1 [62], which was employed for the assembly of genome-based transcripts.

Gene function annotation was meticulously conducted by aligning the protein sequences to the Swiss-Prot database using BLASTP v2.2.28, with a stringent E-value $\leq 1e-5$ [63]. InterProScan v5 [64] was used to annotate the motifs and domains via searches against publicly available databases, including PROSITE [65], Pfam [66], PRINTS [67], PANTHER [68], SMRT [69], and ProDom [70]. This comprehensive approach allowed for the assignment of Gene Ontology (GO) [71] identifiers to genes, correlating them with specific InterPro entries for a nuanced understanding of gene functions. Additionally, protein functions were inferred by leveraging annotation data from the closest matches found in the Swiss-Prot [72] and NR [73] databases, following a BLAST search with an E-value threshold of $< 1e-5$. The Kyoto Encyclopedia of Genes and Genomes (KEGG) [74] database further augmented gene set annotations, providing a pathway-level perspective of gene functions.

For the comprehensive annotation of non-coding RNAs (ncRNAs), tRNAscan-SE version 1.23 [75] was utilized to identify tRNAs, while other ncRNA types were discerned through alignment against the RFAM database version 12.0 [76], using INFERNAL version 1.1.2 [77]. This dual-faceted approach ensures a thorough annotation of both protein-coding and non-coding elements within the *D. delphis* genome.

Gene family, phylogenetic analysis, and divergence time estimation

In this study, we selected 7 species from the Odontoceti group, 8 species from the Mysticeti group, and *Ovis aries* as an outgroup for our phylogenetic analysis, ensuring a broad representation across the evolutionary tree previously constructed for these cetacean groups [78, 79]. The complete genome sequences and annotations of *O. aries*, *P. macrocephalus*, *T. truncatus*, *D. leucas*, *Neophocaena asiaorientalis*, *Lipotes vexillifer*, *Eubalaena glacialis*, *Balaena mysticetus*, *Balaenoptera acutorostrata*, *Balaenoptera musculus*, *Balaenoptera physalus*, *Megaptera novaeangliae*, and *Eschrichtius robustus* were acquired from the NCBI and DNA Zoo databases (Table S1). For the genomic data of *Balaenoptera brydei*, *Grampus griseus*, and *T. aduncus*, we relied on datasets made available by their publishers [80]. Prior to incorporating these datasets into our analysis, we meticulously verified the credibility of these sources and performed additional quality assessments to guarantee the integrity of the data. The time calibration points were based on data sourced from the Timetree website (<http://www.timetree.org/>) and four taxa (*Ovis aries*, *Odontoceti*, *Delphinidae*, and *Balaenopteridae*), which were used to calibrate the

molecular clock in our phylogenetic analysis (Table S2). For detailed procedures including gene family identification, phylogenetic analysis, and divergence time estimation, along with the specific software used, please refer to the respective sections in the Supplementary Materials and Methods.

Expansive, contractive, and rapidly evolving gene families

CAFÉ v4.2 [81] with the default parameters was employed to systematically analyze the expansion and contraction within the gene families of *D. delphis*. Changes within gene families were deemed statistically significant for *p*-values less than 0.05, and highly significant for *p*-values less than 0.01, highlighting gene families undergoing notable evolutionary shifts. To elucidate the biological implications of gene family dynamics in *D. delphis*, GO and KEGG [74] were used to perform functional enrichment analyses on both expanded and contracted gene families. Gene families exhibiting rapid evolution, identified through *p*-values < 0.05 , were further characterized with functional annotations provided by eggNOG-mapper2. These annotations were subsequently analyzed for enrichment patterns using ClusterProfiler v.4 [82].

Detection of positively selected genes

The identification of positively selected genes (PSGs) in the common dolphin was accomplished through the application of the CodeML v4.9 module within the Phylogenetic Analysis by Maximum Likelihood (PAML) software suite [83]. For other detailed methods and software, please refer to the supplementary materials and methods.

Homology analysis

To investigate the homology between *D. delphis* (2n=22) and its sister species, *T. truncatus* (2n=22), we conducted a chromosomal-level pairwise comparison. This comparison encompassed both coding genes and the entire genome, utilizing JCVI v1.1.22 [84] for coding genes and Mummer v4.0.0rc1 [85] for whole-genome comparison. The detailed methods can be found in the supplementary materials and methods.

Demographic history reconstruction

The PSMC (pairwise sequentially Markovian coalescent) method v0.6.5-r67 [86] was used to reconstruct the demographic history of *D. delphis*. Firstly, Samtools and bcftools, called with “samtools mpileup -C30” and “vcftools.pl vcf2fq -d 10 -D 100”, were used to construct diploid genome references. Then the history of changes in the *D. delphis* effective population size were inferred by PSMC with the parameters “-N25 -t15 -r5 -p “4+25*2+4+6””, as in Warren et al. (2017) [87]. The estimated generation

time (g) was set to 9.23 [15] and the mutation rate per generation per site (μ) was 1.5×10^{-8} [78].

Results

Genome size estimation, assembly, and annotation

The genome of a stranded *D. delphis* was sequenced using Illumina and Pacbio technologies. After quality control, we obtained 84.2 Gb Illumina short reads (Table S3). The total number of 17-mers was 75,216,715,516, and the K-mer depth was 29 (Table S4). Therefore, the genome size was estimated at 2569.25 Mb using Jellyfish (Table S4). A subsequent estimation with GenomeScope2 closely matched this at 2,558.37 Mb (Fig. S1). After data processing, a total 80.8 Gb of high-fidelity (HiFi) reads with an average length of 14,404 bp was retained for subsequent analysis (Table S5). The assembly resulted in 266 contigs with a total length of 2,559.1 Mb and a contig N50 of 63.85 Mb. These contigs were organized into 23 chromosomes, including X and a partial Y chromosomes, achieving an anchoring rate of 93.81% (Table 1; Fig. 1A). Finally, the chromosome-level genome assembly covered a total length of 2,400.79 Mb, demonstrating a high level of continuity (Table 1). Moreover, the genome assembly metrics for *D. delphis* were compared with those of *T. truncatus*, as presented in Table 1.

Table 1 Comparative Genome Assembly Metrics for *D. delphis* and *T. truncatus*

| | Metrics | <i>D. delphis</i> | <i>T. truncatus</i> |
|----------------------------|---|-------------------|---------------------|
| Genome assembly statistics | Contig total length | 2,559.1 Mb | 2,372.3 Mb |
| | Number of contigs | 266 | 1036 |
| | Number of scaffolds | 187 | 362 |
| | Maximum contig length | 137.3 Mb | 58.3 Mb |
| | Maximum scaffold length | 183.5 Mb | 183.74 Mb |
| | N50 length (contigs) | 63.9 Mb | 9.7 Mb |
| | N50 length (scaffolds) | 108.9 Mb | 108.4 Mb |
| Genome characteristics | Guanine-cytosine (GC) content | 41.92% | 41.44% |
| | Predicted heterozygosity | 0.33% | 0.27% |
| | Content of repeat sequences | 41.78% | 34.80% |
| | Predicted protein-coding gene number | 22,148 | 18,465 |
| | Average exons of predicted protein-coding genes | 7.92 | 9.88 |
| | Predicted non-coding RNA gene number | 44,085 | 12,372 |
| | Quantity of assembled scaffolds anchored on chromosomes | 23 | 22 |
| | Length of scaffolds anchored on chromosomes | 2,400.8 Mb | 2408.3 Mb |
| | Chromosome number | 23 | 22 |
| | Total number of predicted genes | 22,148 | 24,128 |

The assembly accuracy was evaluated using a library of short reads, which showed a high mapping rate of 99.69% against the assembled genome. This was complemented by a coverage rate of 99.96% and an average sequencing depth of 32.60 \times (Table S6). Notably, only 828 (3.3e-05%) homologous SNPs were detected after mapping the short reads back to the assembled genome, indicating a high level of sequence accuracy (see Table S7). Further analysis revealed that the assembled genome contained 14,874,703 bp of collapsed bases, representing a low collapse rate of 0.58% (detailed in Fig. S2). Moreover, Merqury calculated a Quality Value (QV) of 49.66, reflecting a high genome completeness of 96.51%. Additionally, to evaluate the completeness of the *D. delphis* genome, CEGMA analysis was employed. This analysis identified that 245 out of the 248 core eukaryotic genes (CEGs), accounting for 98.79% completeness, were present in our assembled genome, as shown in Table S8. It is pertinent to note that the term 'Prots' in Table S8 denotes these assembled core genes, underscoring the robustness of our genomic assembly in capturing essential protein-coding sequences representative of eukaryotic life. According to the BUSCO analysis, our genome assembly contains 9,226 genes, with a completeness of 91.0% for the genome and 90.0% for the gene model (Table S9, Fig. S3). Additionally, the analysis identified that 41.78% of the genome assembly, or roughly 1,069.10 Mb, is comprised of repeat sequences (Table 1). The majority of these repeats are long terminal repeats (LTRs) and long interspersed nuclear elements (LINEs), constituting 30.72% and 18.96% of the transposable elements, respectively (Table S10).

The genome assembly predicts a total of 22,148 genes, of which 21,364 (96.50%) have been functionally annotated using various gene databases (Tables 1 and 2). Additionally, we have identified a significant number of non-coding RNAs, including 24,996 miRNAs, 16,963 tRNAs, 252 rRNAs, and 1,874 snRNAs (Table S11). Remarkably, 22,137 of the predicted genes, or 99.95%, are mapped to chromosomes. This comprehensive mapping is depicted in Fig. 1B. The gene density analysis across the 23 chromosomes reveals variation from 5.41 genes/Mb on chromosome 18 to 20.27 genes/Mb on chromosome 19, with an overall average density of 9.22 genes/Mb (Fig. 1B; Table S12).

Phylogenetic and divergence analyses

In this study, we analyzed gene families across 16 whale species and one sheep species, serving as an outgroup, identifying a total of 23,443 gene families. Of these, 5,939 gene families are common to all examined species (Table S13). Notably, *D. delphis* possesses 32 unique gene families, comprising 69 genes that are not found in any other species under study (Table S13). Phylogenetic analysis,

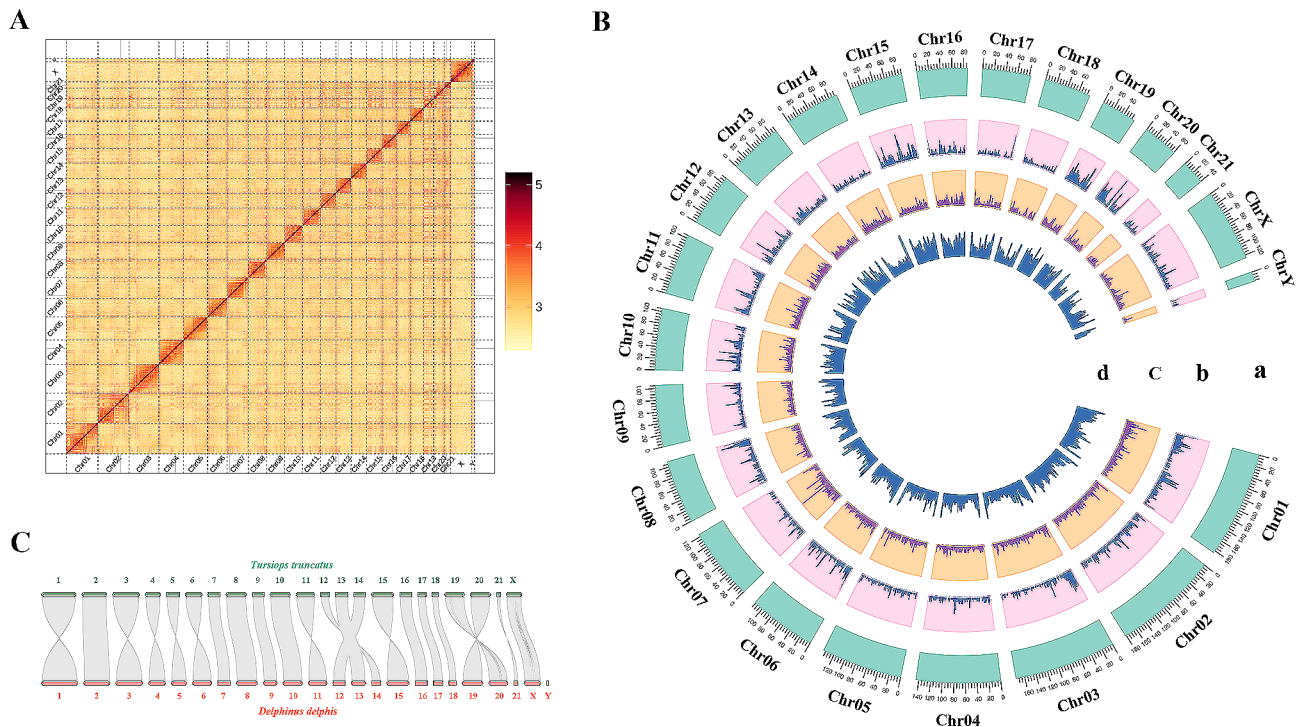


Fig. 1 Genome assembly, synteny, and Circos atlas of *D. delphis*. **(A)** Log₁₀-scaled Hi-C interaction heat map of chromatin in *D. delphis* whole genome, indicating interaction intensity by color depth. **(B)** Circos diagram of the genetic information structure of *D. delphis*. From the outer circle to the inner circle: a, chromosome length information; b, gene density mapping results; c, repeat sequence density; d, GC content. **(C)** Genome synteny between *D. delphis* and *T. truncatus*

Table 2 Summary of functional annotations for predicted genes

| | Number | Percentage (%) |
|-------------|--------|----------------|
| Total | 22,148 | 100 |
| Swiss-Prot | 19,204 | 86.70 |
| Nr | 20,320 | 91.70 |
| KEGG | 17,576 | 79.40 |
| InterPro | 21,026 | 94.90 |
| GO | 14,000 | 63.20 |
| Pfam | 16,843 | 76.00 |
| Annotated | 21,364 | 96.50 |
| Unannotated | 784 | 3.50 |

based on 2,630 single-copy genes, constructed through maximum likelihood estimation, positions *D. delphis* closely with *T. aduncus* and *T. truncatus*, members of the subfamily Delphininae. Subsequently, these species form a cluster with *G. griseus* of the subfamily Globicephalinae (Fig. 2). The divergence timeline suggests that *D. delphis* and the *Tursiops* species parted ways approximately 3.9 million years ago, in the mid-Pliocene era. Moreover, their common ancestor diverged from *G. griseus* roughly 7.1 million years ago, during the late Miocene period (Fig. 2). This study thus offers an in-depth look into the phylogenetic relationships and divergence timelines within Cetacea (Fig. 2).

Specific gene family evolution in *D. Delphis*

In our analysis, we identified 428 expanded and 1,885 contracted gene families in *D. delphis* (Fig. 2). Notably, 80 gene families exhibited significant expansion, while 54 showed significant contraction ($p < 0.01$) (Fig. 2). These expansions and contractions of gene families are assessed relative to their common ancestors with adjacent species, including *T. truncatus* and *T. aduncus*. Further analysis through KEGG pathway enrichment revealed that contracted gene families predominantly associate with biological processes such as gap junction, alpha-linolenic acid metabolism, linoleic acid metabolism and phagosome (Fig. S4). In contrast, significantly expanded gene families were involved in the RIG-I-like receptor signaling pathway (ko04622), JAK-STAT signaling pathway, natural killer cell mediated cytotoxicity and cytokine-cytokine receptor interaction, etc. (KEGG, Fig. S5). Among the expanded gene families, three were highlighted for their potential pivotal roles in *D. delphis*' biological functions, as evidenced by KEGG enrichment analysis (Fig. S5).

We identified 14 HSP70 (K03283, Hsp70) family genes scattered across 8 chromosomes and three contigs within the *D. delphis* genome (Fig. 3A). Abundant pairs of HSP70 gene segmental duplicates were found in the genome (Fig. 3B, Table S14). In contrast to *T. truncatus*, which possesses 5 HSP70 family members, *D. delphis*

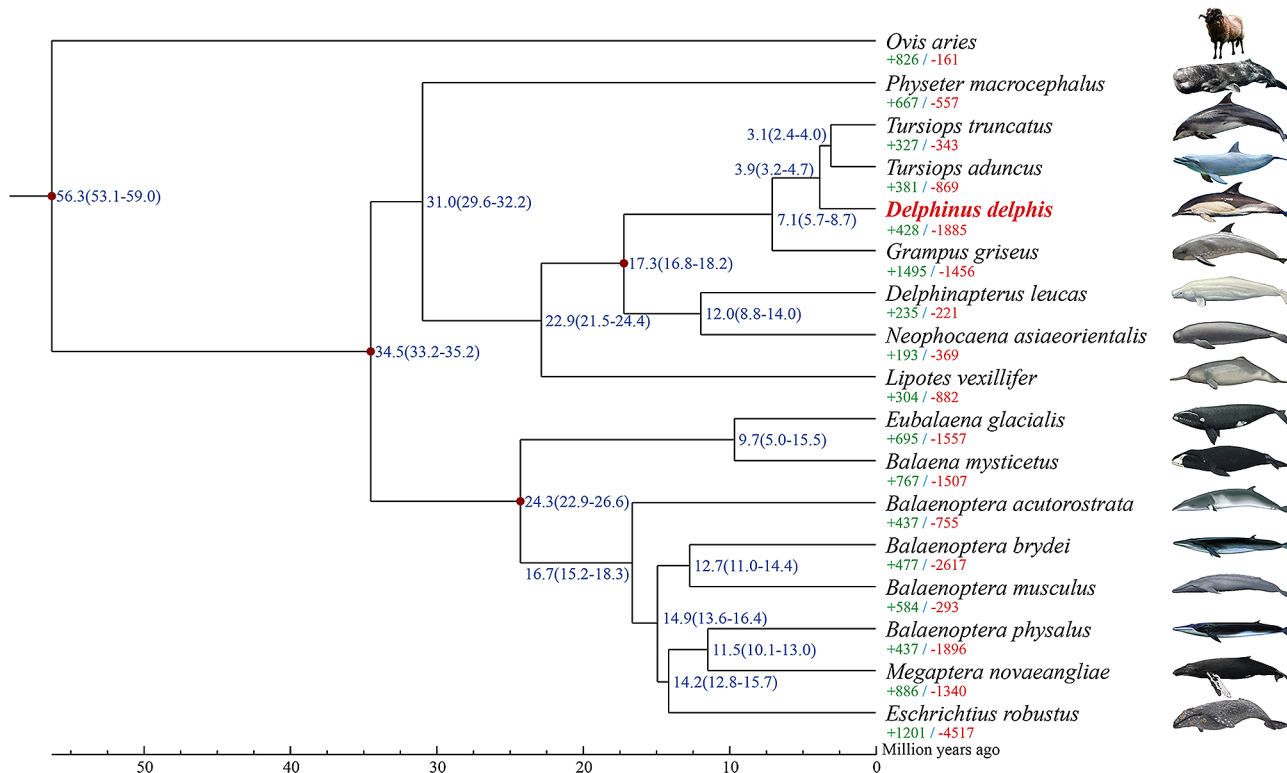


Fig. 2 Maximum likelihood phylogenetic analysis of *D. delphis* and other cetaceans with *Ovis aries* outgroup. Each branch site shows the estimated species divergence time (million years ago). The majority of the branches exhibit a branch support of 100. A notable exception is the branching point leading to *Eschrichtius robustus* and the common ancestor of both *B. physalus* and *Megaptera novaeangliae*, which has a branch support of 94. The green numbers indicate the number of gene families that expanded during the evolution of the species and the red numbers indicate the number of gene families that contracted. The sources of species images are provided in Table S1

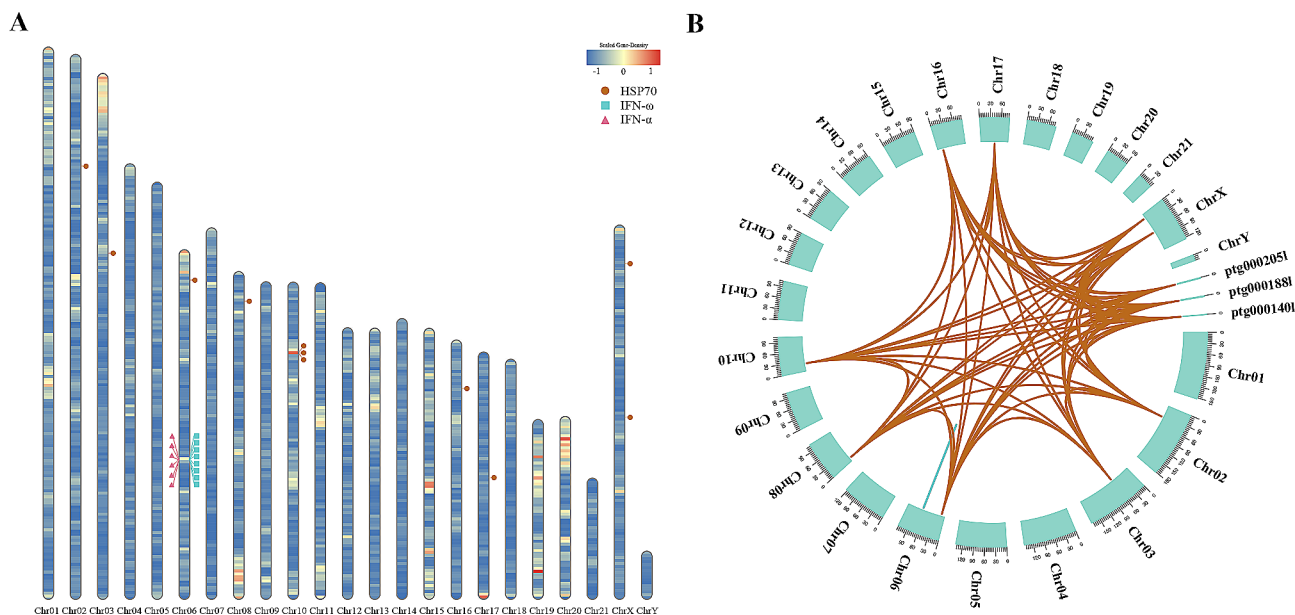


Fig. 3 Distributions and sequence identity of three expanded gene families in the genome of *D. delphis*. **(A)** Chromosomal distribution of HSP70, IFN- α , and IFN- ω genes in *D. delphis*, with color-coded gene density (genes/Mb) heat map. **(B)** Sequence identity of the HSP70, IFN- α , and IFN- ω genes in the genome of *D. delphis*

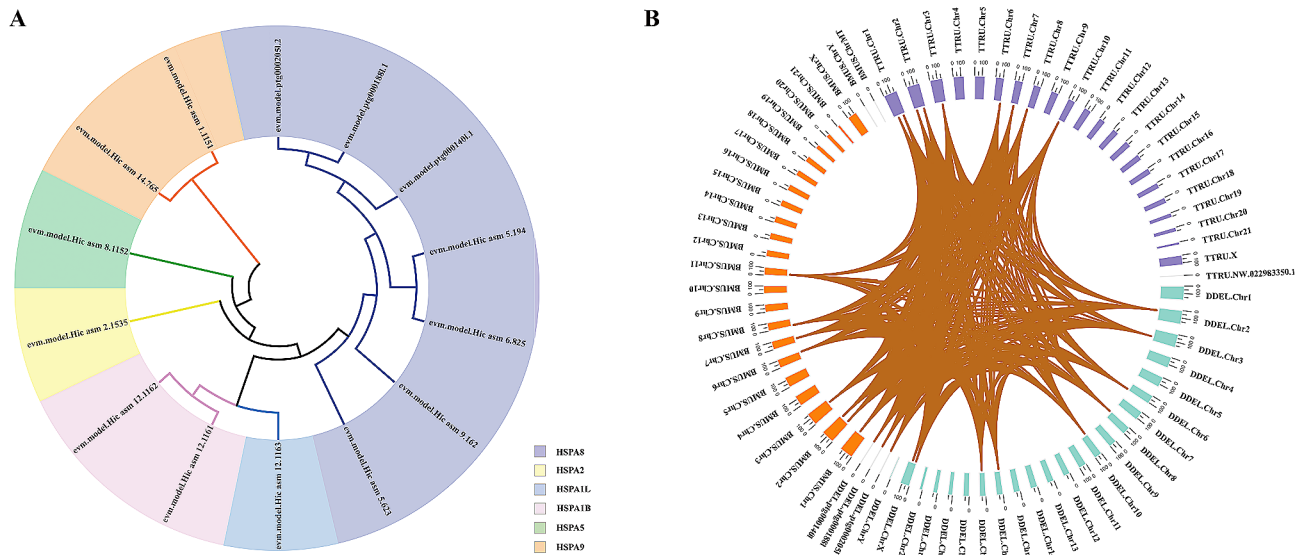


Fig. 4 Phylogenetic and synteny analysis of HSP70 genes. **(A)** Maximum likelihood phylogenetic tree constructed using HSP70 genes in *D. delphis*. Gene identifiers, such as “evm.model.Hic asm 9.162”, are used to label specific genes within the HSP70 family. **(B)** Synteny analysis of HSP70 genes among *D. delphis*, *T. truncatus*, and *B. musculus*. The color tags represent species identifiers: blue green for *D. delphis* (DDEL), purple for *T. truncatus* (TTRU), and orange for *B. musculus* (BMUS). Notations like “Chr1” are used to indicate chromosome numbers

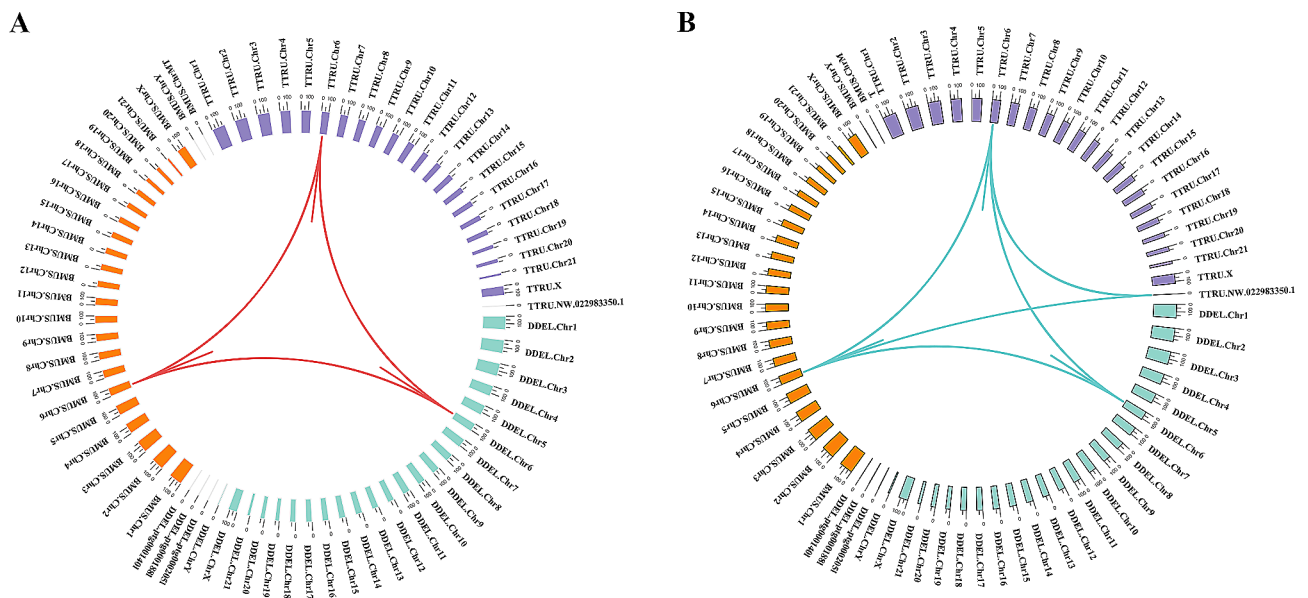


Fig. 5 Synteny analysis and expression profiling of IFN- α and IFN- ω genes. **(A)** Synteny analysis of IFN- α genes among *D. delphis*, *T. truncatus*, and **(B)** *B. musculus*. The abbreviations “DDEL”, “TTRU”, and “BMUS” represent *D. delphis*, *T. truncatus*, and *B. musculus*, respectively. Notations like “Chr1” are used to indicate chromosome numbers. **B.** Synteny analysis of IFN- ω genes among the three aforementioned species

exhibits a richer diversity with these genes segregating into 6 distinct subgroups. This classification was based on an in-depth phylogenetic analysis and examination of motif compositions (Fig. 4A, Fig. S6). Moreover, the collinearity analysis between *D. delphis* and the two representative species, *T. truncatus* and *B. musculus*, highlighted numerous homologous HSP70 gene pairs present within the syntenic regions (Fig. 4B). Notably, *D. delphis* shows a unique distribution pattern, with half

of its HSP70 genes falling within the HSPA8 subgroup (Fig. 4A), a proportion that stands in contrast to *T. truncatus* (40%) and *B. musculus* (22%) (Fig. S6).

According to our results, we discerned a specific clustering of interferon genes within the *D. delphis* genome, locating 6 IFN- α (K05414, IFNA) and 8 IFN- ω (K05440, IFNW) genes primarily on chromosome 6 (Fig. 3A). The genes of the IFN- α and IFN- ω families exhibited fairly high sequence identity (Fig. 3B, Table S15, Table S16). In

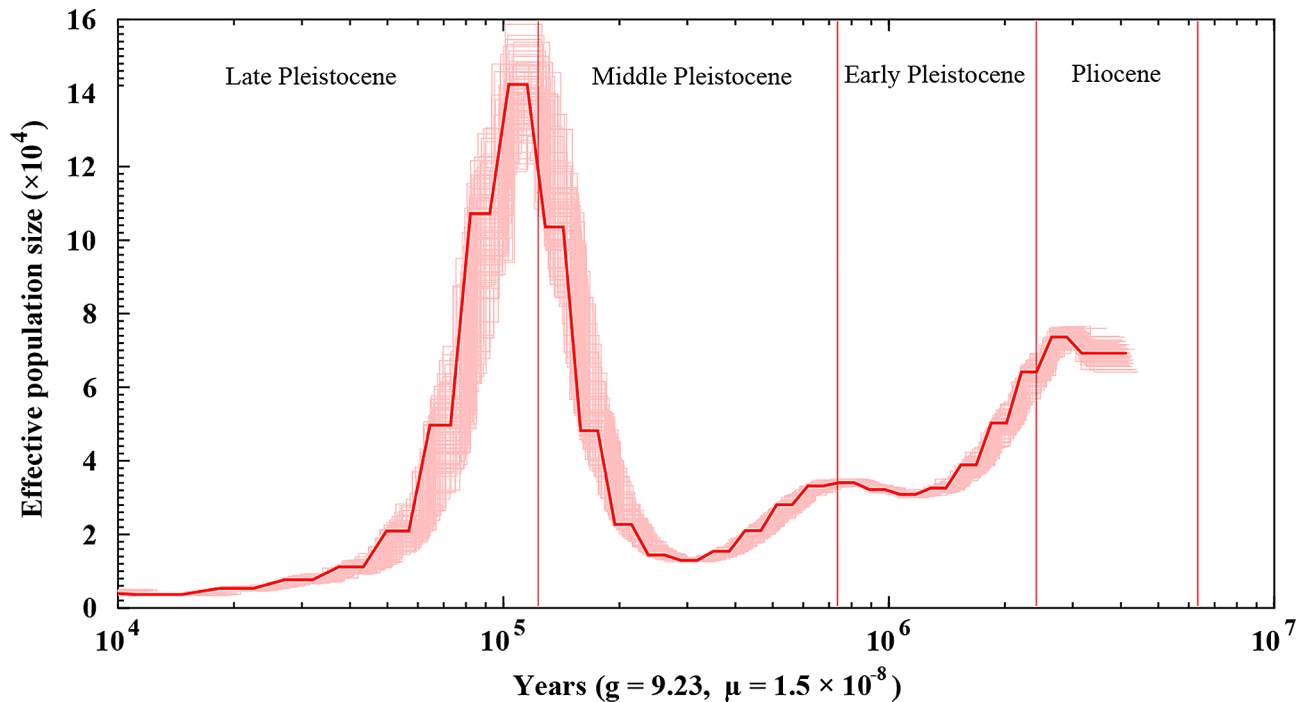


Fig. 6 Historical effective population size of *D. delphis* based on PSMC analysis. The thick red line represents the primary PSMC estimate from the original genomic data. The light red lines indicate bootstrap replicates to reflect the variability and robustness of the PSMC estimates

addition, in the synteny analyses, 3 and 6 pairs of homologous genes from the IFN- α and IFN- ω gene families, respectively, were present within the syntenic regions among the genomes of *D. delphis*, *T. truncatus*, and *B. musculus* (Fig. 5A, B). Further phylogenetic and motif analysis led to the categorization of *D. delphis*' IFN- α and IFN- ω genes into distinct subgroups: IFN- α 1, IFN- α 2, IFN- α 3 for IFN- α , and IFN- ω 1, IFN- ω 2 for IFN- ω (Fig. S7, Fig. S8).

Genes under positive selection

In our study, we identified 120 genes under positive selection, as indicated by a false discovery rate (FDR) of less than 0.05. Through comprehensive KEGG pathway enrichment analysis [81], these genes predominantly contribute to several key biological processes, including histidine metabolism, the FoxO signaling pathway, riboflavin metabolism, the RIG-I-like receptor signaling pathway, sulfur metabolism, ubiquinone and other terpenoid-quinone biosynthesis (Fig. S9). Notably, three of these genes—tripartite motif-containing protein 25 (K10652, TRIM25), peptidyl-prolyl cis-trans isomerase NIMA-interacting 1 (K09578, PIN1), and p38 MAP kinase (K04441, p38)—emerged as critical components of the RIG-I-like receptor signaling pathway, underscoring their potential pivotal roles in adaptive responses.

Demographic history

The effective population size (N_e) of *D. delphis* ranged from 0.4×10^4 to 14.2×10^4 during the period of 4000 ~ 10 Ka (Fig. 6). The PSMC indicated there was a substantial population decrease from 7.5×10^4 to 1.2×10^4 during the early Pleistocene age and the first half of the middle Pleistocene age (320,000–2,430,000 years ago) (Fig. 6). After that, the population of common dolphins increased sharply to its peak in the early upper Pleistocene age (about 120,000 years ago) and then decreased drastically to its minimum at the end of the upper Pleistocene age (about 10,000 years ago) (Fig. 6).

Discussion

Quality and significance of *D. Delphis* genome assembly

Our assembly of the *D. delphis* genome showcases outstanding quality, underscored by the minimal homologous SNPs identified upon re-mapping the short reads to the assembled genome, thereby implying a remarkably low error rate. Such precision aligns with the current upward trend in cetacean genome assembly quality [88], marking a significant stride in the field. Notably, the assembly's Quality Value (QV) stands at an impressive 49.66, highlighting the assembly's accuracy and the genome's detailed representation. When compared to the genome of *T. truncatus*, the *D. delphis* assembly not only boasts a greater contig N50 length but also encompasses a wider array of predicted non-coding RNA genes (Table 1). This comparison serves to underline the depth

and comprehensiveness of our genomic assembly, illustrating its substantial contribution to cetacean genomics.

The notable synteny observed between the genomes of *D. delphis* and *T. truncatus* underscores the evolutionary stability prevalent within the Delphinidae family (Fig. 1C). This pattern of synteny is not unique to these two species, it has also been identified in the genomes of other cetaceans, including the rough-toothed dolphin (*Steno bredanensis*) and the melon-headed whale (*Peponocephala electra*), underscoring a broader trend of evolutionary conservation among cetacean species [89]. The high-quality genome assembly of *D. delphis* introduced in this research thus emerges as a crucial asset for comparative genomic studies aimed at unraveling the ecological and evolutionary dynamics that shape the Delphinidae family.

Evolutionary relationships and genomic conservation in *D. Delphis*

The discernment of a modest quantity of gene families exclusive to *D. delphis* indicates an evolutionary distinctiveness, notwithstanding a significant genomic conservation among the cetaceans analyzed. The molecular phylogenetic analysis, showcasing a close kinship between *D. delphis* and the *Tursiops* species (*T. aduncus* and *T. truncatus*), aligns with prior classifications derived from RADseq data [78]. This alignment underscores the efficacy of utilizing diverse genomic methodologies for elucidating cetacean phylogenies. The estimated divergence times, pinpointing the evolutionary separation of *D. delphis* from its nearest kin in the Pliocene and Miocene epochs, shed light on the adaptive and evolutionary trajectories of common dolphins throughout these periods. Additionally, the congruence of our findings with earlier research based on targeted sequence capture [79] reinforces the dependability and consistency of phylogenetic reconstructions in cetaceans.

Adaptive evolution of key gene families in *D. Delphis*

The expansion and contraction of gene families play pivotal roles in the evolution of adaptive traits [90]. Notably, the pronounced contraction of gene families associated with gap junctions and fatty acid metabolism, coupled with the expansion in gene families involved in signaling and immune response pathways, suggests specific evolutionary pressures and adaptation strategies in *D. delphis*. These observations emphasize the significance of gene family dynamics in unraveling evolutionary paths and potential adaptive strategies. Moreover, the discovery of three specifically expanded gene families, deemed to have substantial functions, points to unique areas of biological significance in *D. delphis*.

Heat shock protein 70 (HSP70) represents a highly conserved gene family with members identified in both

prokaryotes and eukaryotes [91–93]. The HSP70 gene family's high conservation, evidenced by abundant segmental duplicates, indicates its evolutionary importance in common dolphins. Conserved syntenic regions shared among *D. delphis*, *T. truncatus*, and *B. musculus* underline the gene family's crucial role in cetacean adaptation. Variations in HSP70 members among these species [94] and their gene distribution hint at species-specific evolutionary adaptations. Notably, the HSPA8 subgroup in *D. delphis* suggests specialized cellular stress response mechanisms.

The expansion of the HSP70 gene family in common dolphins likely aids their adaptation to environmental changes like hypoxia, temperature shifts, and pH variations. HSP70 genes are vital for cellular protection against stress and promoting cell survival [91, 95, 96]. HSP70 proteins can buffer against diverse cellular stresses, including elevated temperature, pH fluctuations, hypoxia, pollutants, and oxidative stress [93, 97]. This might be related to their broad distribution [1, 2], ability to dive to extreme depths, travel long distances, and highly mobility [4, 7]. Diverse *D. delphis* populations show significant genomic variation in coasts with fluctuating sea conditions [8]. Such genetic traits likely underscore their adaptability to intricate marine habitats.

The expansion of the HSP70 gene family might also contribute to the *D. delphis*' longevity and resistance to accumulated pollutants. Dolphins, notably *D. delphis* with lifespans up to 30 years [6, 14], exhibit exceptional longevity [98]. Cellular stress resistance in animals is correlated with longevity [99], with enhanced resistance being vital for longer-lived species [100, 101]. A strong correlation between HSP70 expression and longer lifespans suggests elevated basal HSP70 levels in longer-lived animals [99]. While a link between longevity and elevated HSP expression is established in various species [99], its specific implication for *D. delphis* remains to be determined. Given cetaceans' status as marine pollution indicators due to pollutant accumulation [12, 102], HSP70 genes' potential in mitigating toxic effects is notable [97, 103].

Interferons (IFNs) are potent cytokines that play a crucial role in the process of innate immune responses, which have shown antiviral, antineoplastic, and anti-inflammatory functions [104, 105]. Type I IFNs (including IFN- α , IFN- β , IFN- ω , etc.) are a class of the three IFN subtypes [106, 107]. The genes of the IFN- α and IFN- ω families in the *D. delphis* genome exhibited a pronounced sequence identity. This conservation, further supported by the presence of homologous gene pairs from the IFN- α and IFN- ω gene families within syntenic regions across *D. delphis*, *T. truncatus*, and *B. musculus*, emphasizes the evolutionary significance of these gene families in cetaceans. The observed conservation may suggest a

conserved function and mechanism of action for these genes across cetaceans. Given the fundamental role of interferons in innate immune responses, such conservation underscores their importance in mediating antiviral and anti-inflammatory responses in cetaceans [108, 109]. IFN genes may be transcriptionally upregulated in response to specific stimuli, such as immune challenges, potentially accounting for their observed low baseline expressions across the surveyed tissues in this study [110].

The expansions in the IFN- α and IFN- ω gene families in the genome of *D. delphis* may indicate strong antiviral, anti-inflammatory, and antineoplastic abilities in common dolphins. IFN- α and IFN- ω are the two most important type I IFNs, and they have particularly potent antiviral, antiproliferative, anti-inflammatory, and immunomodulatory properties [108, 109]. IFN- α is a key cytokine in the innate immune response induced by infections and tissue stress and damage [104]. It is generated by fibroblasts and T- and NK-cells [111] to combat unrecognized organisms and cells, including viruses and tumor cells [104]. Clinically, IFN- α is used to prevent or treat different viral infections [112, 113] and it also produces beneficial effects in several tumor-associated diseases [114, 115]. In addition, IFN- ω is secreted primarily by virus-infected leukocytes and has been identified in numerous mammalian groups [116, 117]. It activates the phosphatidylinositol-3-kinase/protein kinase B (P13K/Akt) signaling pathway to up-regulate antiviral activity [118, 119]. Compared with IFN- α , IFN- ω is more effective in inhibiting virus replication and has exhibited some degree of cross-species activity [120, 121]. Furthermore, it has been shown to have anti-proliferation and antitumor effects [107].

Implications of genes under positive selection in immune and antitumor mechanisms

Positively selected genes often reflect evolutionary adaptations to specific environmental challenges or physiological needs [122]. In the context of our study, three such genes emerged as particularly intriguing due to their involvement in the RIG-I-like receptor signaling pathway, which is pivotal for the recognition of viral pathogens and the modulation of innate immune responses. The first, TRIM25, is an E3 ubiquitin ligase enzyme that regulates the K63-linked ubiquitination of RIG-I, which is essential for RIG-I downstream signaling and the innate immune response to viral infections [123]. TRIM25 also modulates cell proliferation and migration [124, 125], apoptosis, and plays a key role in tumorigenesis [126, 127]. Previous studies revealed that TRIM25 is under positive selection pressure in primates [128, 129]. The second, PIN1, is a member of the parvulin family that modulates a large subset of key oncogenes and tumor suppressors

by catalyzing the cis/trans isomerization of specific pSer/Thr-Pro motifs [130, 131]. PIN1 facilitates the functions of multiple oncogenes and abrogates tumor suppressors [132], and hence its deregulation results in disease, especially cancer [133]. Humans with genetic polymorphisms that reduce PIN1 expression have a lower risk for multiple cancers [134, 135]. Similarly, PIN1 knockout mice are highly resistant to tumorigenesis, even amid the overexpression of oncogenes [136, 137]. Besides, PIN1 also plays a role in inflammatory diseases and viral infections [130]. The third, p38, is one of the four main subgroups of mitogen-activated protein kinases (MAPKs) [138]. It is involved in numerous complex biological processes, including cell proliferation, cell differentiation, cell death, cell apoptosis, cell migration, and cell invasion [138, 139]. Its pathways can be activated in response to a variety of environmental and cellular stresses, such as inflammation and tumorigenesis, among other signals [140, 141].

According to the properties and functions of these three genes in the RIG-I-like receptor signaling pathway, which are under positive selection pressures, they may also be related to the anti-inflammatory and antitumor mechanisms [142] in *D. delphis*. As cetaceans are a long-lived class of mammals, they should have already developed antitumor mechanisms [143]. A variety of tumor suppressor genes (TSGs) have been investigated in cetaceans before, and their positive selection and gene duplication provided some insight into how cetaceans resist cancers [143]. Many TSGs are involved in cellular proliferation, differentiation, and apoptosis [144], and are related to diseases, especially cancers [145, 146].

Historical population dynamics and influencing factors in *D. Delphis*

The estimation of the historical effective population size is intrinsically tied to our understanding of the species' evolutionary history [147]. As it provides insights into the past population size of the species and how historical events, such as environmental changes, hybridization, migration, or disease outbreaks, have impacted the population [148]. Compared with other cetaceans such as *T. truncatus*, *T. aduncus*, *B. acutorostrata*, etc [78, 149].., the population of *D. delphis* experienced larger (or abnormal) contractions and expansions during the Pleistocene. This divergence in demographic history is consistent with our phylogenetic findings, suggesting that *D. delphis*, *T. truncatus*, and *T. aduncus* have a common ancestor but have experienced distinct evolutionary trajectories. Our genomic data supports the notion that these population dynamics in *D. delphis* are not only unique but also a key component in understanding its evolutionary history. One previous study estimated that *D. delphis* originated in the Pacific Ocean of the Northern Hemisphere [150], and a cooling of the tropical Pacific during the

Pleistocene may have driven them to disperse across equatorial waters to the Southern Hemisphere [151, 152]. Simultaneously, new niches would be opened due to the changes in primary productivity and prey abundance [153], which might have facilitated the colonization of common dolphins around the world. Indeed, there were rapid climatic changes and oceanographic shifts during the mid-Pleistocene, and the subsequent stage of high productivity in the Pacific Ocean, owed to a major cooling event [152, 154], might have led to a drastic increase of N_e in this species. The rapid reduction in N_e that followed might have resulted from a subsequent decrease in productivity due to higher temperatures [150]. On the other hand, common dolphins are known to hybridize with other dolphins [155, 156], hence the dramatic fluctuations in their effective population size estimated by genomic data might also be induced by substantial genetic exchange with *D. delphis* through hybridization during the Pleistocene [149].

Conclusions

Here, we presented a high-quality genome of the common dolphin *D. delphis* with 2.56 Gb and 93.81% of contigs anchored onto 23 chromosomes. Genomic comparisons showed that *D. delphis* is closely related to *T. truncatus* and *T. aduncus*, and diverged ca. 3.9 MYA. The expansions of the HSP70, IFN- α , and IFN- ω gene families, and the positively selected genes encoding TRIM 25, PIN1, and p38, might underlie the evolutionary success of common dolphins. These data also indicated drastic contractions and expansions of the effective population size of *D. delphis* during the Pleistocene. This high-quality genome data represents significant new resources for cetacean and mammalian studies.

Supplementary Information

The online version contains supplementary material available at <https://doi.org/10.1186/s12864-024-10268-4>.

Supplementary Material 1

Supplementary Material 2

Supplementary Material 3

Acknowledgements

We sincerely thank the Administration of Ocean and Fisheries of Fujian for the assistance during sample collection.

Author contributions

X-l Z, X-y W, and Q-z X conceived the study. K D, Q-z X, and L-y Z wrote the manuscript. K D, Q-z X, X-l Z, L-y Z, Y-x L, Z L, Q-h Z, and X-y W revised the manuscript. L-y Z, Q-h Z, and X-y W performed sample preparation. Q-z X, W-g S, Y-x L, and Z L performed the experiment. K D and Q-z X performed the analysis.

Funding

This study was supported by the China-ASEAN Maritime Cooperation Fund, the National Natural Science Foundation of China (NO. 42176135, 42076159), and the Fujian Provincial Natural Science Foundation (2021J06031).

Data availability

The datasets presented in this study are available in the NCBI Sequence Read Archive under the accession number PRJNA903213, <https://www.ncbi.nlm.nih.gov/datasets/taxonomy/9728/>.

Declarations

Ethics approval and consent to participate

The sampling of the dolphin carcass in this study was authorized by the Fishery Administration of Fujian Province, China. No specific permit number was issued as our research was for the stranded dolphins but not live animals, which did not involve human biomedical research mentioned in the Declaration of Helsinki. Our sample collection procedures adhered to the 'Regulations of the People's Republic of China for the Implementation of Wild Aquatic Animal Protection' (promulgated in 1993). We declare that our research complies with the guidelines for animal care and scientific experiments in China.

Consent to publish

Not applicable.

Competing interests

The authors declare no competing interests.

Received: 15 March 2023 / Accepted: 28 March 2024

Published online: 16 April 2024

References

- Evans W. Common dolphin, white-bellied porpoise *Delphinus delphis* Linnaeus, 1758. *Handb Mar Mamm*. 1994;5:191–224.
- Hammond P, Bearzi G, Bjørge A, Forney K, Karczmarski L, Kasuya T, Perrin W, Scott M, Wang J, Wells R. *Delphinus delphis*. The IUCN Red List of Threatened Species 2008: e.T6336A12649851. In.; 2008.
- Moura AE, Sillero N, Rodrigues A. Common dolphin (*Delphinus delphis*) habitat preferences using data from two platforms of opportunity. *Acta Oecol*. 2012;38:24–32.
- Paradell OG, López BD, Methion S. Modelling common dolphin (*Delphinus delphis*) coastal distribution and habitat use: insights for conservation. *Ocean Coastal Manage*. 2019;179:104836.
- Hui CA. Power and speed of swimming dolphins. *J Mammal*. 1987;68(1):126–32.
- Viallelle S. Dolphins and Whales from the Azores. IGS 2002:pp 18.
- Möller L, Valdez FP, Allen S, Bilgmann K, Corrigan S, Beheregaray LB. Fine-scale genetic structure in short-beaked common dolphins (*Delphinus delphis*) along the East Australian Current. *Mar Biol*. 2011;158:113–26.
- Barceló A, Sandoval-Castillo J, Brauer CJ, Bilgmann K, Parra GJ, Beheregaray LB, Möller LM. Seascape genomics of common dolphins (*Delphinus delphis*) reveals adaptive diversity linked to regional and local oceanography. *BMC Ecol Evol*. 2022;22(1):1–18.
- De Pierrepont J, Dubois B, Desormonts S, Santos M, Robin J. Stomach contents of English Channel cetaceans stranded on the coast of Normandy. *J Mar Biol Association United Kingd*. 2005;85(6):1539–46.
- Young DD, Cockcroft VG. Diet of common dolphins (*Delphinus delphis*) off the south-east coast of southern Africa: opportunism or specialization? *Proceedings of the Zoological Society of London* 2010, 234(1):41–53.
- Murphy S, Pierce GJ, Law R, Bersuder P, Jepson P, Learmonth J, Addink M, Dabin W, Santos M, Deaville R. Assessing the effect of persistent organic pollutants on reproductive activity in common dolphins and harbour porpoises. *J Northwest Atl Fish Sci*. 2010;42:153–73.
- Borrell A, Cantos G, Pastor T, Aguilar A. Organochlorine compounds in common dolphins (*Delphinus delphis*) from the Atlantic and Mediterranean waters of Spain. *Environ Pollut*. 2001;114(2):265–74.

13. Lahaye V, Bustamante P, Dabin W, Churlaud C, Caurant F. Trace element levels in foetus–mother pairs of short-beaked common dolphins (*Delphinus delphis*) stranded along the French coasts. *Environ Int.* 2007;33(8):1021–8.
14. Boness D, Clapham PJ, Mesnick SL. Life history and reproductive strategies. *Mar Mammal Biology: Evolutionary Approach* 2002:278–324.
15. Mannocci L, Dabin W, Augeraud-Véron E, Dupuy J-F, Barbraud C, Ridoux V. Assessing the impact of bycatch on dolphin populations: the case of the common dolphin in the eastern North Atlantic. *PLoS ONE.* 2012;7(2):e32615.
16. Murphy S, Collet A, Rogan E. Mating strategy in the male common dolphin (*Delphinus delphis*): what gonadal analysis tells us. *J Mammal.* 2005;86(6):1247–58.
17. Murphy S, Winship A, Dabin W, Jepson PD, Deaville R, Reid RJ, Spurrier C, Rogan E, López A, González AF. Importance of biological parameters in assessing the status of *Delphinus delphis*. *Mar Ecol Prog Ser.* 2009;388:273–91.
18. Gui D, Jia K, Xia J, Yang L, Chen J, Wu Y, Yi M. De novo assembly of the Indo-Pacific humpback dolphin leucocyte transcriptome to identify putative genes involved in the aquatic adaptation and immune response. *PLoS one* 2013(8):e72417.
19. Ohishi K, Shishido R, Iwata Y, Saitoh M, Takenaka R, Ohtsu D, Okutsu K, Maruyama T. Lipopolysaccharide-induced innate immune factors in the bottlenose dolphin (*Tursiops truncatus*) detected in expression sequence tag analysis. *Microbiol Immunol.* 2011;55(11):790–7.
20. Beineke A, Siebert U, Wohlsein P, Baumgärtner W. Immunology of whales and dolphins. *Vet Immunol Immunopathol.* 2010;133(2–4):81–94.
21. Kemper CM, Tomo I, Bingham J, Bastianello SS, Wang J, Gibbs SE, Woolford L, Dickason C, Kelly D. Morbillivirus-associated unusual mortality event in South Australian bottlenose dolphins is largest reported for the Southern Hemisphere. *Royal Society open science* 2016(12):160838.
22. Batley KC, Sandoval-Castillo J, Kemper CM, Zanardo N, Tomo I, Beheregaray LB, Möller LM. Whole genomes reveal multiple candidate genes and pathways involved in the immune response of dolphins to a highly infectious virus. *Mol Ecol.* 2021;30(23):6434–48.
23. Newman S, Smith SA. Review article: Marine mammal neoplasia: a review. *Vet Pathol.* 2006;43(6):865–80.
24. Jaber JR, Pérez J, Carballo M, Arbelo M, Monteros A, Herráez P, Muñoz J, Andrada M, Rodríguez F, Fernández A. Hepatosplenic large cell immunoblastic lymphoma in a Bottlenose Dolphin (*Tursiops truncatus*) with high levels of Polychlorinated Biphenyl congeners. *J Comp Pathol.* 2005;132(2–3):242–7.
25. Martineau D, Lemberger K, Dallaire A, Labelle P, Mikaelian I. Cancer in wildlife, a case study: beluga from the St. Lawrence Estuary, Québec, Canada. *Environ Health Perspect.* 2002;110(3):285–92.
26. Martineau D, Lair S, Guise SD, Liscomb TP, Beland P. Cancer in beluga whales from the St Lawrence Estuary, Quebec, Canada: a potential biomarker of environmental contamination. *J Cetacean Res Manage.* 1999;1(1):249–65.
27. De Guise S, Martineau D, Béland P, Fournier M. Possible mechanisms of action of environmental contaminants on St. Lawrence beluga whales (*Delphinapterus leucas*). *Environ Health Perspect.* 1995;103(suppl 4):73–7.
28. Theissinger K, Fernandes C, Formenti G, Bista I, Berg PR, Bleidorn C, Bombarely A, Crottini A, Gallo GR, Godoy JA. How genomics can help biodiversity conservation. *Trends in Genetics;* 2023.
29. Fan G, Chen J, Jin T, Shi C, Du X, Zhang H, Zhang Y, Li H, Luo T, Yan P. The report of marine life genomic research. 2018.
30. Fan G, Zhang Y, Liu X, Wang J, Sun Z, Sun S, Zhang H, Chen J, Lv M, Han K. The first chromosome-level genome for a marine mammal as a resource to study ecology and evolution. *Mol Ecol Resour.* 2019;19(4):944–56.
31. Bian C, Huang Y, Li J, You X, Yi Y, Ge W, Shi Q. Divergence, evolution and adaptation in ray-finned fish genomes. *Sci China Life Sci.* 2019;62:1003–18.
32. Ravi V, Venkatesh B. The divergent genomes of teleosts. *Annual Rev Anim Biosci* 2018(No.1):47–68.
33. Morin PA, Alexander A, Blaxter M, Caballero S, Fedrigo O, Fontaine M, Foote A, Maloney B, McCarthy M, McGowen MR. Building genomic infrastructure: sequencing platinum-standard reference-quality genomes of all cetacean species. *Mar Mamm Sci.* 2020;36(4):1356–66.
34. Pugliares KR, Bogomolni A, Touhey KM, Herzig SM, Harry CT. Marine mammal necropsy: an introductory guide for stranding responders and field biologists. 2007.
35. Zhang C, Song Z, Wthornton S, Dong E, Cao P, Ye F, Wang X, Zhang Y. Ultrasound beam shift induced by short-beaked common dolphin's (*Delphinus delphis*) tissues as an attenuating gradient material. Volume 64. *Science China Physics, Mechanics & Astronomy;* 2021. p. 108711. 10.
36. Belton J-M, McCord RP, Gibcus JH, Naumova N, Zhan Y, Dekker J. Hi-C: a comprehensive technique to capture the conformation of genomes. *Methods.* 2012;58(3):268–76.
37. Liu B, Shi Y, Yuan J, Hu X, Zhang H, Li N, Li Z, Chen Y, Mu D, Fan W. Estimation of genomic characteristics by analyzing *k*-mer frequency in de novo genome projects. *In;* 2013: 62–7.
38. Guillaume Marçais, Carl K. A fast, lock-free approach for efficient parallel counting of occurrences of *k*-mers. *Bioinformatics* 2011.
39. Ranallo-Benavidez TR, Jaron KS, Schatz MC. GenomeScope 2.0 and Smudgeplot for reference-free profiling of polyploid genomes. *Nat Commun.* 2020;11(1):1432.
40. Zhang X, Zhang S, Zhao Q, Ming R, Tang H. Assembly of allele-aware, chromosomal-scale autopolyploid genomes based on Hi-C data. *Nat Plants.* 2019;5(8):833–45.
41. Roach MJ, Schmidt SA, Borneman AR. Purge Haplotigs: allelic contig reassignment for third-gen diploid genome assemblies. *BMC Bioinformatics.* 2018;19(1):1–10.
42. Langmead B, Wilks C, Antonescu V, Charles R. Scaling read aligners to hundreds of threads on general-purpose processors. *Bioinformatics.* 2019;35(3):421–32.
43. Wingett S, Ewels P, Furlan-Magaril M, Nagano T, Schoenfelder S, Fraser P, Andrews S. HiCUP: pipeline for mapping and processing Hi-C data. *F1000Research* 2015, 4.
44. Zhang J, Zhang X, Tang H, Zhang Q, Hua X, Ma X, Zhu F, Jones T, Zhu X, Bowers J. Allele-defined genome of the autopolyploid sugarcane *Saccharum spontaneum* L. *Nat Genet.* 2018;50(11):1565–73.
45. Howe K, Chow W, Collins J, Pelan S, Pointon D-L, Sims Y, Torrance J, Tracey A, Wood J. Significantly improving the quality of genome assemblies through curation. *Gigascience.* 2021;10(1):giaa153.
46. Blanco E, Parra G, Guigó R. Using geneid to identify genes. *Curr Protocols Bioinf.* 2007;18(1):431–4328.
47. Manni M, Berkeley MR, Seppey M, Simão FA, Zdobnov EM. BUSCO update: novel and streamlined workflows along with broader and deeper phylogenetic coverage for scoring of eukaryotic, prokaryotic, and viral genomes. *Mol Biol Evol* 2021(No.10):4647–54.
48. Li H. Minimap2: pairwise alignment for nucleotide sequences. *Bioinformatics.* 2018;34(18):3094–100.
49. Li H, Handsaker B, Wysoker A, Fennell T, Ruan J, Homer N, Marth G, Abecasis G, Durbin R, Subgroup GPDP. The sequence alignment/map format and SAMtools. *Bioinformatics.* 2009;25(16):2078–9.
50. Rhie A, Walenz BP, Koren S, Phillippy AM. Merqury: reference-free quality, completeness, and phasing assessment for genome assemblies. *Genome Biol.* 2020;21(1):1–27.
51. Benson G. Tandem repeats finder: a program to analyze DNA sequences. *Nucleic Acids Res.* 1999;27(2):573–80.
52. Tarailo-Graovac M, Chen N. Using RepeatMasker to identify repetitive elements in genomic sequences. *Curr Protocols Bioinf* 2009, 25(1).
53. Bao W, Kojima KK, Kohany O. Repbase Update, a database of repetitive elements in eukaryotic genomes. *Mob Dna.* 2015;6:1–6.
54. Zhao X. W Hao 2007 LTR_FINDER: an efficient tool for the prediction of full-length LTR retrotransposons. *Nucleic Acids Res* 35 Web Server issue W265–268.
55. Price AL, Jones NC, Pevzner PA. De novo identification of repeat families in large genomes. *Bioinformatics* 2005(suppl_1):i351.
56. Cantarel BL, Korfi I, Robb SM, Parra G, Ross E, Moore B, Holt C, Alvarado AS, Yandell M. MAKER: an easy-to-use annotation pipeline designed for emerging model organism genomes. *Genome Res.* 2008;18(1):188–96.
57. Burge C, Karlin S. Prediction of complete gene structures in human genomic DNA. *J Mol Biol.* 1997;268(1):78–94.
58. Majoros W, Pertea M, Salzberg S. TigrScan and GlimmerHMM: two open source ab initio eukaryotic gene-finders. *Bioinformatics.* 2004;20(16):2878–9.
59. Altschul SF, Gish W, Miller W, Myers EW, Lipman DJ. Basic local alignment search tool. *J Mol Biol.* 1990;215(3):403–10.
60. Birney E, Clamp M, Durbin R. GeneWise and genomewise. *Genome Res.* 2004;14(5):988–95.
61. Pertea M, Kim D, Pertea GM, Leek JT, Salzberg SL. Transcript-level expression analysis of RNA-seq experiments with HISAT, StringTie and Ballgown. *Nat Protoc.* 2016;11(9):1650–67.
62. Ghosh S, Chan C-KK. Analysis of RNA-Seq data using TopHat and Cufflinks. *Plant Bioinformatics: Methods Protocols* 2016:339–61.
63. Scott MG, Madden TL. BLAST: at the core of a powerful and diverse set of sequence analysis tools. *Nucleic Acids Research (suppl_2):*W20.

64. Jones P, Binns D, Chang HY, Fraser M, Li W, McAnulla C, McWilliam H, Maslen J, Mitchell A, Nuka G. InterProScan 5: genome-scale protein function classification. *Bioinformatics*. 2014;30(9):1236–40.
65. Hulo N, Bairoch A, Bulliard V, Cerutti L, De Castro E, Langendijk-Genevaux PS, Pagni M, Sigrist CJ. The PROSITE database. *Nucleic Acids Res*. 2006;34(suppl1):D227–30.
66. Finn RD, Jaina M, John T, Penny C, Andreas H, Pollington JE, Luke GO, Prasad G, Goran C, Kristoffer F. The Pfam protein families database. *Nucleic Acids Res*. 2000;28(1).
67. Attwood TK, Bradley P, Flower DR, Gaulton A, Maudling N, Mitchell AL, Moulton G, Nordle A, Paine K, Taylor P. PRINTS and its automatic supplement, prePRINTS. *Nucleic Acids Res*. 2003;31(1):400–2.
68. Mi H, Betty LU, Rozina L, Anish K, Jody V, Steven R, Guo N, Anushya M, Olivier D, Campbell MJ. The PANTHER database of protein families, subfamilies, functions and pathways. *Nucleic Acids Res*. 2005(suppl_1):D284.
69. Ponting CP, Jrg S, Frank M, Peer B. SMART: identification and annotation of domains from signalling and extracellular protein sequences. *Nucleic Acids Res*. 1999(1):229–32.
70. Ashburner M, Ball CA, Blake JA, Botstein D, Butler H, Cherry JM, Davis AP, Dolinski K, Dwight SS, Eppig JT. Gene ontology: tool for the unification of biology. *Nat Genet*. 2000;25(1):25–9.
71. Bru C, Courcelle E, Carrère S, Beausse Y, Dalmar S, Kahn D. The ProDom database of protein domain families: more emphasis on 3D. *Nucleic Acids Res*. 2005;33(suppl1):D212–5.
72. UniProt. Reorganizing the protein space at the Universal Protein Resource (UniProt). *Nucleic Acids Res*. 2012(Suppl):D71–5.
73. Pruitt KD, Tatiana T, Brown GR, Maglott DR. NCBI reference sequences (RefSeq): current status, new features and genome annotation policy. *Nucleic Acids Res*. 2012(D1):D130–5.
74. Kanehisa M, Goto S. KEGG: kyoto encyclopedia of genes and genomes. *Nucleic Acids Res*. 2000(No.1):27–30.
75. Schattner P, Brooks AN, Lowe TM. The tRNAscan-SE, snoscan and snoGPS web servers for the detection of tRNAs and snoRNAs. *Nucleic Acids Res*. 2005;33(Web Server issue):686–9.
76. Nawrocki EP, Burge SW, Bateman A, Daub J, Eberhardt RY, Eddy SR, Floden EW, Gardner PP, Jones TA, Tate J et al. Rfam 12.0: updates to the RNA families database. *Nucleic Acids Res*. 2015(D1):D130–7.
77. Chen C, Chen H, Zhang Y, Thomas HR, Frank MH, He Y, Xia R. TBtools: an integrative toolkit developed for interactive analyses of big biological data. *Mol Plant*. 2020;13(8):1194–202.
78. Moura AEa K, Tf et al. Möller Lg, Natoli Ah, Gaspari Si, McGowen Mj Phylogenomics of the genus *Tursiops* and closely related *Delphininae* reveals extensive reticulation among lineages and provides inference about eco-evolutionary drivers(Article). *Molecular Phylogenetics and Evolution*: 2020:106756.
79. McGowen MR, Tsagkogeorga G, Álvarez-Carretero S, Reis Md, Struebig M, Deaville R, Jepson PD, Jarman S, Polanowski A, Morin PA et al. Phylogenomic resolution of the Cetacean Tree of Life using Target sequence capture. *Syst Biol*. 2020(No.3):479–501.
80. Yuan Y, Yaolei Z, Peijun Z, Chang L, Jiahao W, Haiyu G, Rus A, Inge H, Meiqi S, Mingli L. L: Comparative genomics provides insights into the aquatic adaptations of mammals. *Proc Natl Acad Sci USA*. 2021(37).
81. De Bie T, Cristianini N, Demuth JP, Hahn MW. CAFE: a computational tool for the study of gene family evolution. *Bioinformatics*. 2006;22(10):1269–71.
82. Yu G, Wang LG, Han Y, He QY. clusterProfiler: an R package for comparing biological themes among gene clusters. *Omics-a J Integr Biology*. 2012;16(5):284–7.
83. Yang Z. PAML 4: phylogenetic analysis by Maximum Likelihood. *Mol Biol Evol*. 2007;24(8):1586–91.
84. Tang H, Bowers JE, Wang X, Ming R, Alam M, Paterson AH. Synteny and Colinearity in Plant genomes. *Science*. 2008;320(5875):486–8.
85. Delcher AL, Salzberg SL, Phillippy AM. Using MUMmer to identify similar regions in large sequence sets. *Current protocols in bioinformatics*. 2003(1):10.13. 11–10.13. 18.
86. Li H, Durbin R. Inference of human population history from individual whole-genome sequences. *Nature*. 2011;475(7355):493.
87. Warren WCa K, Lb A, Ac C, Jd. Pérez-Silva JGe, López-Otín Ce, Quesada Ve, Minx Pa, Tomlinson Ca, Montague MJF: The Novel Evolution of the Sperm Whale Genome. *Genome Biology and Evolution*. 2017(No.12):3260–3264.
88. Zhang P, Zhao Y, Li C, Lin M, Dong L, Zhang R, Liu M, Li K, Zhang H, Liu X. An Indo-Pacific humpback dolphin genome reveals insights into chromosome evolution and the demography of a vulnerable species. *Iscience*. 2020;23(10).
89. Gao H, Kang H, Zhang Y, Wang J, Lin W, Zhang P, Lin M, Liu M, Fan G, Li S. Chromosome-Level Genome Assembly of the rough-toothed Dolphin (*Steno bredanensis*). *J Mar Sci Eng*. 2023;11(2):418.
90. Hahn WM. Estimating the tempo and mode of gene family evolution from comparative genomic data. *Genome Res*. 2005(No.8):1153–60.
91. Albakova Z, Armeev GA, Kanevskiy LM, Kovalenko EI, Sapozhnikov AM. HSP70 multi-functionality in cancer. *Cells*. 2020;9(3):587.
92. Zhu X, Zhao X, Burkholder WF, Gragerov A, Ogata CM, Gottesman ME, Hendrickson WA. Structural analysis of substrate binding by the molecular chaperone DnaK. *New York, NY: Science*; 1996. pp. 1606–14. No.5268.
93. Murphy ME. The HSP70 family and cancer. *Carcinogenesis*. 2013(6):1181–8.
94. Junprung W, Norouzitallab P, Vos SD, Tassanakajon A, Viet DN, Stappen GV, Bossier P. Sequence and expression analysis of HSP70 family genes in *Artemia franciscana*. *Nat Publishing Group*. 2019(1).
95. Beere HM, Green DR. Stress management—heat shock protein-70 and the regulation of apoptosis. *Trends Cell Biol*. 2001;11(1):6–10.
96. Daugaard M, Rohde M, Jäättelä M. The heat shock protein 70 family: highly homologous proteins with overlapping and distinct functions. *FEBS Lett*. 2007;581(19):3702–10.
97. Jia K, Ding L, Zhang L, Zhang M, Yi M, Wu Y. In Vitro Assessment of Environmental Stress of Persistent Organic Pollutants on the Indo-Pacific Humpback Dolphin. *Toxicology in vitro: an international journal published in association with BIBRA*. 2015(No.1Part B):529–35.
98. Gunn-Moore D, Kaidanovich-Bellin O, Iradi MCG, Gunn-Moore F, Lovestone S. Alzheimer's disease in humans and other animals: a consequence of postreproductive life span and longevity rather than aging. *Alzheimer's Dement*. 2018;14(2):195–204.
99. Salway KD, Gallagher EJ, Page MM, Stuart JA. Higher levels of heat shock proteins in longer-lived mammals and birds. *Mech Ageing Dev*. 2011;132(6–7):287–97.
100. Kapahi P, Boulton M, Kirkwood T. Positive correlation between mammalian life span and cellular resistance to stress. *Free Radic Biol Med*. 1999(No.5–6):495–500.
101. Kirkwood T, Kapahi P, Shanley DP. Evolution, stress, and longevity. *J Anat*. 2010;197(4):587–90.
102. Zhou JL, Salvador SM, Liu YP, Sequeira M. Heavy metals in the tissues of common dolphins (*Delphinus delphis*) stranded on the Portuguese coast. *Sci Total Environ*. 2001;273(1):61–76.
103. Wang L, Liang XF, Huang Y, Li SY, Ip KC. Transcriptional responses of xenobiotic metabolizing enzymes, HSP70 and Na⁺/K⁺-ATPase in the liver of rabbitfish (*Siganus oramin*) intracoelomically injected with amnesic shellfish poisoning toxin. *Environ Toxicol*. 2008.
104. Lombardi A, Tsomos E, Hammarstad SS, Tomer Y. Interferon alpha: the key trigger of type 1 diabetes. *J Autoimmun*. 2018;94:7–15.
105. Khanmohammadi S, Rezaei N, Khazaei M, Shirvani A. A case of autosomal recessive interferon alpha/beta receptor alpha chain (IFNAR1) deficiency with severe COVID-19. *J Clin Immunol*. 2022:1–6.
106. Wang Y, Jiang S, Jiang X, Sun X, Guan X, Han Y, Zhong L, Song H, Xu Y. Cloning and codon optimization of a novel feline interferon omega gene for production by *Pichia pastoris* and its antiviral efficacy in polyethylene glycol-modified form. *Virulence*. 2022;13(1):297–309.
107. Li SF, Zhao FR, Shao JJ, Xie YL, Zhang YG. Interferon-omega: current status in clinical applications. *Int Immunopharmacol*. 2017;52:253–60.
108. MinayoshiaÅ Y, MaedaaÅ H, Yanagisawaa H, Hamasakia K, Mizutaa Y. Development of Kupffer cell targeting type-I interferon for the treatment of hepatitis via inducing anti-inflammatory and immunomodulatory actions. *Drug Delivery*. 2018;25(1):1067–77.
109. Gerlach N, Schimmer S, Weiss S, Kalinke U, Dittmer U. Effects of type I interferons on friend retrovirus infection. *J Virol*. 2006;80(7):3438–44.
110. De Weerd NA, Nguyen T. The interferons and their receptors—distribution and regulation. *Immunol Cell Biol*. 2012;90(5):483–91.
111. Schaefer M, Engelbrecht MA, Gut O, Fiebich BL, Lieb K. Interferon alpha (IFN?) And psychiatric syndromes: a review. *Prog Neuro-psychopharmacol Biol Psychiatry*. 2002;26(4):731–46.
112. Asselah T, Lada O, Moucari R, Martinot M, Boyer N, Marcellin P. Interferon therapy for chronic hepatitis B. *Clinics in liver disease*. 2007;11(4):839–49.
113. Brinkmann V, Geiger T, Alkan S, Heusser CH. Interferon alpha increases the frequency of interferon gamma-producing human CD⁴⁺ T cells. *J Exp Med*. 1993;178(5):1655–63.
114. Guttermann JJ. Leukocyte Interferon-Induced Tumor Regression in Human metastatic breast Cancer, multiple myeloma, and Malignant Lymphoma. *Ann Intern Med*. 1980;93(3):399–406.

115. Zilberstein A, Ruggieri R, Revel M. The Interferon System. 1985.
116. Detournay O, Morrison DA, Wagner B, Zarnegar B, Watrang E. Genomic analysis and mRNA expression of equine type I interferon genes. *J Interferon Cytokine Res.* 2013;33(12):746–59.
117. Sang Y, Rowland RRR, Hesse RA. Differential expression and activity of the porcine type I interferon family. *Physiol Genom* 2010(2):248–58.
118. Klarquist J, Cantrell R, Lehn M, Lampe K, Hennies C, Hoebe K, Janssen E. Type I IFN drives experimental systemic lupus erythematosus by distinct mechanisms in CD4 T cells and B cells. *ImmunoHorizons.* 2020;4(3):140–52.
119. Seo Y, Kim M, Choi, Minjoung, Sunhee, Park, Kidae, Iljung: possible role of Phosphoinositide-3-Kinase in Mx1 protein translation and antiviral activity of Interferon-Omega-stimulated HeLa cells. *Pharmacology.* 2011;87(3–4):224–31.
120. de Mari K, Maynard L, Sanquer A, Lebreux B, Eun HM. Therapeutic effects of recombinant feline interferon-co on feline leukemia virus (FeLV)-Infected and FeLV/feline immunodeficiency virus (FIV)-coinfected symptomatic cats. *J Vet Intern Med.* 2004;18(4):477–82.
121. Leal RO, Gil S, Duarte A, Mcgahie D, Sepúlveda N, Niza MMRE, Tavares L. Evaluation of viremia, proviral load and cytokine profile in naturally feline immunodeficiency virus infected cats treated with two different protocols of recombinant feline interferon omega. *Res Vet Sci.* 2015;99:87–95.
122. Chebii VJ, Oyola SO, Kotze A, Domelevo Entfellner J-B, Musembi Mutuku J, Agaba M. Genome-wide analysis of nubian ibex reveals candidate positively selected genes that contribute to its adaptation to the desert environment. *Animals.* 2020;10(11):2181.
123. Lin H, Jiang M, Liu L, Yang Z, Ma Z, Liu S, Ma Y, Zhang L, Cao X. The long non-coding RNA *Lnczc3h7a* promotes a TRIM25-mediated RIG-I antiviral innate immune response. *Nat Immunol* 2019.
124. Dai H, Zhang P, Zhao S, Zhang J, Wang B. Regulation of the vascular endothelial growth factor and growth by estrogen and antiestrogens through Efp in Ishikawa endometrial carcinoma cells. *Oncol Rep.* 2009;21(2):395–401.
125. Heikel G, Choudhury NR, Michlewski G. The role of Trim25 in development, disease and RNA metabolism. *Biochem Soc Trans.* 2016;44(4):1045–50.
126. Li F, Sun Q, Liu K, Zhang L, Zhao W. OTUD5 cooperates with TRIM25 in transcriptional regulation and tumor progression via deubiquitination activity. *Nat Commun.* 2020;11(1):4184.
127. Martin-Vicente M, Medrano LM, Resino S. TRIM25 in the regulation of the antiviral innate immunity. *Front Immunol* 2017:1187.
128. Han K, Lou DI, Sawyer SL. Identification of a genomic reservoir for new TRIM genes in primate genomes. *PLoS Genet.* 2011;7(12):e1002388.
129. Ray MB, Sawyer SL, Wu LI, Michael E, Malik HS. An evolutionary screen highlights canonical and noncanonical candidate antiviral genes within the Primate TRIM Gene Family. *Genome Biology and Evolution*, 5,11(2013-10-24) 2013(11):2141–54.
130. Xue H, Liu H, Xu L, Liu Q, Zhuo B, Dai M, Wu Z, Chen M, Chen Q. Serum peptidyl-prolyl cis-trans isomerase NIMA-interacting 1 in combination with C-reactive protein and white blood cell as novel predictors for infants with community-acquired pneumonia. *Eur J Inflamm* 2020.
131. Shingo Kozono1, Lin Y-M 3 et al. H-S, Benika Pinch3, Xiaolan Lian1, 5,6, Chenxi Qiu1, 7, Megan K. Herbert1, Chun-Hau Chen1, Tan3 L, Ziang Jeff Gao1 Arsenic targets Pin1 and cooperates with retinoic acid to inhibit cancer-driving pathways and tumor-initiating cells. *Nature Communications:* 2018.
132. Nakatsu Y, Yamamotoya T, Ueda K, Ono H, Inoue MK, Matsunaga Y, Kushiyama A, Sakoda H, Fujishiro M, Matsubara A. Prolyl isomerase Pin1 in metabolic reprogramming of cancer cells. *Cancer letters* 2020(470-):470.
133. Kim G, Bhattarai PY, Choi HS. Peptidyl-prolyl cis/trans isomerase NIMA-interacting 1 as a molecular target in breast cancer: a therapeutic perspective of gynecological cancer. *Archives Pharmacol Res* 2019(No2):128–39.
134. Lu KP. Prolyl isomerase Pin1 as a molecular target for cancer diagnostics and therapeutics. *Cancer Cell.* 2003;4(3):175–80.
135. Lu Z, Hunter T. Prolyl isomerase Pin1 in cancer. *Cell Res* 2014.
136. D'Artista L, Bisso A, Piontini A, Doni M, Verrecchia A, Kress TR, Morelli MJ, Del Sal G, Amati B, Campaner S. Pin1 is required for sustained B cell proliferation upon oncogenic activation of myc. *Oncotarget.* 2016;7(16):21786.
137. Wulf G, Garg P, Liou YC, Iglehart D, Lu KP. Modeling breast cancer in vivo and ex vivo reveals an essential role of Pin1 in tumorigenesis. *EMBO J.* 2014;23(16):3397–407.
138. Koul HK, Pal M, Koul S. Role of p38 MAP Kinase Signal Transduction in Solid tumors. *Genes cancer* 2013(No.9–10):342–59.
139. Dubey D, Srivastav AK, Singh J, Chopra D, Qureshi S, Kushwaha HN, Singh N, Ray RS. Photoexcited triclosan induced DNA damage and oxidative stress via p38 MAP kinase signaling involving type I radicals under sunlight/UVB exposure. *Ecotoxicol Environ Saf.* 2019;174:270–82.
140. Zarubin T, Han J. Activation and signaling of the p38 MAP kinase pathway. *Cell Res.* 2005;15(1):11–8.
141. Zhang YL, Dong C. MAP kinases in immune responses. *Cell Mol Immunol.* 2005;2(1):20–7.
142. Song J, Li M, Li C, Liu K, Zhu Y, Zhang H. Friend or foe: RIG-I like receptors and diseases. *Autoimmun rev* 2022:103161.
143. Tejada-Martinez D, Magalhes JPD, Opazo JC. Positive selection and gene duplications in tumour suppressor genes reveal clues about how cetaceans resist cancer. *Proceedings Biological sciences* 2021, 288(1945):20202592.
144. Guo C, Liu S, Sun MZ. Potential role of ANXA1 in cancer. *Future Oncol.* 2013;9(11):1773–93.
145. Cui T, Chen Y, Yang L, Knösel T, Zöller K, Huber O, Petersen I. DSC3 expression is regulated by p53, and methylation of DSC3 DNA is a prognostic marker in human colorectal cancer. *Br J Cancer.* 2011;104(6):1013–9.
146. Oshiro MM, Kim CJ, Wozniak RJ, Junk DJ, Muñoz-Rodríguez JL, Burr JA, Fitzgerald M, Pawar SC, Cress AE, Domann FE et al. Epigenetic silencing of DSC3 is a common event in human breast cancer. *Breast Cancer Res* 2005(No.5):R669–80.
147. Nadachowska-Brzyska K, Burri R, Smeds L, Ellegren H. PSMC analysis of effective population sizes in molecular ecology and its application to black-and-white Ficedula flycatchers. *Mol Ecol.* 2016;25(5):1058–72.
148. Garcia-Berro A, Talla V, Vila R, Wai HK, Shipilina D, Chan KG, Pierce NE, Backström N, Talavera G. Migratory behaviour is positively associated with genetic diversity in butterflies. *Mol Ecol.* 2023;32(3):560–74.
149. Yim1 H-S, Cho2 YS, Guang3 X, Sung Gyun Kang1, Jae-Yeon Jeong1, Sun-Shin Cha1, 5, Oh1 H-M, Lee1 J-H, Yang1 EC, Kae Kyoung Kwon1: Minke whale genome and aquatic adaptation in cetaceans. *Nat Genet* 2014(No.1):88–92.
150. Amaral AR, Beheregaray LB, Bilgmann K, Freitas L, Robertson KM, Sequeira M, Stockin KA, Coelho M, Möller LM. Influences of past climatic changes on historical population structure and demography of a cosmopolitan marine predator, the common dolphin (genus *Delphinus*). *Mol Ecol.* 2012;21(19):4854–71.
151. Lee SY, Poulsen CJ. Tropical Pacific climate response to obliquity forcing in the Pleistocene. *Paleoceanography Paleoclimatology.* 2005;20(4):–.
152. Lawrence KT, Liu Z, Herbert TD. Evolution of the eastern tropical Pacific through Plio-Pleistocene glaciation. *Science.* 2006;312(5770):79–83.
153. Harlin-Cognato AD, Markowitz T, Würsig B, Honeycutt RL. Multi-locus phylogeography of the dusky dolphin (*Lagenorhynchus obscurus*): passive dispersal via the west-wind drift or response to prey species and climate change? *BMC Evol Biol.* 2007;7(1):1–17.
154. Morley JJ, Dworetzky BA. Evolving pliocene-pleistocene climate: a North Pacific perspective. *Q Sci Rev.* 1991;10(2):225–37.
155. Antoniou A, Frantzis A, Alexiadou P, Paschou N, Poulakakis N. Evidence of introgressive hybridization between *Stenella coeruleoalba* and *Delphinus delphis* in the Greek seas. *Mol Phylogenet Evol.* 2018;129:325–37.
156. Espada R, Olaya-Ponzzone L, Haasova L, Martín E, García-Gómez JC. Hybridization in the wild between *Tursiops truncatus* (Montagu 1821) and *Delphinus delphis* (Linnaeus 1758). *PLoS ONE.* 2019;14(4):e0215020.

Publisher's Note

Springer Nature remains neutral with regard to jurisdictional claims in published maps and institutional affiliations.